



HAL
open science

Bambus[4,6]urils as dual scaffolds for multivalent iminosugar presentation and ion transport: access to unprecedented glycosidase-directed anion caging agents

Marine Lafosse, Yan Liang, Jérémy P Schneider, Elise Cartier, Anne Bodlenner, Philippe Compain, Marie-Pierre Heck

► To cite this version:

Marine Lafosse, Yan Liang, Jérémy P Schneider, Elise Cartier, Anne Bodlenner, et al.. Bambus[4,6]urils as dual scaffolds for multivalent iminosugar presentation and ion transport: access to unprecedented glycosidase-directed anion caging agents. *Molecules*, 2022, 27 (15), pp.4772-10.3390/molecules27154772 . cea-04361621

HAL Id: cea-04361621

<https://cea.hal.science/cea-04361621v1>

Submitted on 22 Dec 2023

HAL is a multi-disciplinary open access archive for the deposit and dissemination of scientific research documents, whether they are published or not. The documents may come from teaching and research institutions in France or abroad, or from public or private research centers.


L'archive ouverte pluridisciplinaire **HAL**, est destinée au dépôt et à la diffusion de documents scientifiques de niveau recherche, publiés ou non, émanant des établissements d'enseignement et de recherche français ou étrangers, des laboratoires publics ou privés.



Distributed under a Creative Commons Attribution - NonCommercial 4.0 International License

Communication

Bambus[4,6]urils as Dual Scaffolds for Multivalent Iminosugar Presentation and Ion Transport: Access to Unprecedented Glycosidase-Directed Anion Caging Agents

Marine Lafosse ¹, Yan Liang ², Jérémy P. Schneider ², Elise Cartier ¹, Anne Bodlenner ^{2,*} , Philippe Compain ^{2,*} and Marie-Pierre Heck ^{1,*}

¹ Département Médicaments et Technologies pour la Santé (DMTS), Université Paris-Saclay, CEA, INRAE, SCBM, 91191 Gif-sur-Yvette, France; marine.lafosse@orange.fr (M.L.); elise.cartier@cea.fr (E.C.)

² Equipe de Synthèse Organique et Molécules Bioactives (SYBIO), Laboratoire d'Innovation Moléculaire et Applications (LIMA), University of Strasbourg | University of Haute-Alsace | CNRS (UMR 7042), 67087 Strasbourg, France; yolandaly168@outlook.com (Y.L.); jeremy.schneider@live.fr (J.P.S.)

* Correspondence: annebod@unistra.fr (A.B.); philippe.compain@unistra.fr (P.C.); marie-pierre.heck@cea.fr (M.-P.H.); Tel.: +33-3-6885-2792 (P.C.); +33-1-6908-3703 (M.-P.H.)

Abstract: Bambusurils, BU[4] and BU[6], were used for the first time as multivalent scaffolds to link glycosidases inhibitors derived from 1-deoxynojirimycin (DNJ). Two linear DNJ ligands having six or nine carbon alkyl azido linkers or a trivalent DNJ dendron were grafted onto octapropargylated BU[4] and dodecapropargylated BU[6] using copper-catalyzed cycloaddition (CuAAC) to yield corresponding neoglycobambus[4] and neoglycobambus[6]urils bearing 8 to 24 iminosugars. The inhibition potencies of neoglycoBU[4], neoglycoBU[6] and neoglycoBU[6] caging anions were evaluated against Jack Bean α -mannosidase and compared to monovalent DNJ derivatives. Strong affinity enhancements per inhibitory head were obtained for the clusters holding trivalent dendrons with inhibitory constants in the nanomolar range ($K_i = 24$ nM for BU[4] with 24 DNJ units). Interestingly, the anion (bromide or iodide) encapsulated inside the cavity of BU[6] does not modify the inhibition potency of neoglycoBU[6], opening the way to water-soluble glycosidase-directed anion caging agents that may find applications in important fields such as bio(in)organic chemistry or oncology.

Keywords: bambusuril; multivalency; iminosugars; CuAAC; enzyme inhibition; DNJ; α -mannosidase



Citation: Lafosse, M.; Liang, Y.; Schneider, J.P.; Cartier, E.; Bodlenner, A.; Compain, P.; Heck, M.-P. Bambus[4,6]urils as Dual Scaffolds for Multivalent Iminosugar Presentation and Ion Transport: Access to Unprecedented Glycosidase-Directed Anion Caging Agents. *Molecules* **2022**, *27*, 4772. <https://doi.org/10.3390/molecules27154772>

Academic Editors: Daniele D'Alonzo, Annalisa Guaragna and Andrea Goti

Received: 29 June 2022

Accepted: 21 July 2022

Published: 26 July 2022

Publisher's Note: MDPI stays neutral with regard to jurisdictional claims in published maps and institutional affiliations.



Copyright: © 2022 by the authors. Licensee MDPI, Basel, Switzerland. This article is an open access article distributed under the terms and conditions of the Creative Commons Attribution (CC BY) license (<https://creativecommons.org/licenses/by/4.0/>).

1. Introduction

Bambus[n]urils, R_{2n} BU[n] ($n = 4, 6$), are synthetic neutral cyclooligomers composed of R_2 disubstituted glycoluril units connected by n -methylene bridges [1]. BU[4,6] show a rigid conformation in an alternate arrangement that looks similar to a double-cup jigger. The well-defined cavity of BU[6] is of ideal size to entrap anions [1–3]. This strong anion-caging property of BU[6] was utilized for anion sensing, [4,5] transport [6,7] and extraction [8–10] as well as in photoinduced electron transfer [11]. However, BU[4], having a smaller internal cavity than BU[6] derivatives, is unable to include any anions and so far does not have any applications. Nevertheless, the modular valency of 8 to 12 for R_8 BU[4] and R_{12} BU[6], respectively, their topology allowing ligands to be grafted on upper and lower rims, their arm flexibility and, even more importantly, their cheap and easy synthesis make BU[4] and BU[6] attractive scaffolds for the construction of multivalent derivatives. We have previously synthesized allylated bambus[4,6]urils that were submitted to thiol–ene click coupling (TEC) with thiosugars to generate the corresponding 8–12 thiosugar-functionalized bambus[4,6]urils [12,13]. As a proof of concept, we recently developed an alternative strategy using propargylated bambus[4,6]urils able to be post-functionalized by click chemistry (CuAAC) so as to afford multivalent architectures bearing 8 or 12 glucose units [14].

In the present work, we report the first examples of multivalent bambus[n]urils–iminosugar conjugates. N -alkyl analogs of 1-deoxynojirimycin (DNJ) were chosen as

inhibitors (inhibiting epitopes) since the best inhibitory multivalent effects were reported with these motifs on Jack Bean α -mannosidase [15–20]. Despite the large number of scaffolds used for multimerization of iminosugar inhibitors [15–26], starting from C₆₀, polyols, cyclodextrins, porphyrins, calixarenes and gold nanoparticles to the most effective cyclopeptides, it is still relevant to study new structures that might have different topologies and contact points with glycosidases together with other physical properties of interest, such as anion binding ability. Indeed, it was shown that the binding modes of Jack Bean α -mannosidases with iminosugar-based multivalent inhibitors not only depend on the nature and number of bioactive inhibitors, but more importantly on the shape and size of the multivalent scaffold as well as ligand density [15–20]. Multimerization of inhibitors proved to be an attractive strategy, enabling valency-corrected inhibition enhancements of up to three [26] to four [27] orders of magnitude, inhibition selectivity refining or enzyme activation [28,29]. Multivalent drugs on nanoparticles also proved efficient for escaping efflux pumps [30]. Originally discovered with glycosidases [15–20], the inhibitory multivalent effect has been generalized to other enzymes such as glycosyltransferases and carbonic anhydrases [31–34]. In the case of enzyme inhibition, multivalent inhibitors may interact with enzymes by numerous mechanisms, such as the bind-and-recapture process, the chelate effect or receptor clustering [15–20,35].

Since anions such as bromide and iodide can easily and strongly be complexed inside BU[6], we have explored whether they would impact the rigidity and shape of the scaffold, and thus possibly the interaction with the model glycosidase used for studying inhibitory multivalent effects. Our objective was to access unprecedented water-soluble glycosidase-directed anion caging agents. Here, we describe the full details of our study, from the synthesis of bambus[*n*]urils–iminosugar conjugates to the quantification of host–guest interaction of these neoglycoclusters with iodide anion and their evaluation as Jack Bean α -mannosidase inhibitors.

2. Results and Discussion

2.1. Preparation of DNJ-Functionalized Bambusuril neoglyco₈BU[4], neoglyco₁₂BU[6] and X@neoglyco₁₂BU[6]

The best multivalent effects in glycosidase inhibition using non-polymeric inhibitors were obtained thanks to a study relying on a gradual increase in cyclopeptide scaffold size and valency, which led to small aggregates between two enzymes and the multimeric inhibitor being highlighted as the best cluster of the series [26,36]. Important click partners of this study were azide-armed N-C6 and N-C9 alkyl DNJ [37] and tripod DNJ derivatives [38]. These building blocks were consequently selected for the synthesis of the first examples of bambus[*n*]urils-based iminosugars **3–11** (Figure 1). Based on our recent results [14], octapropargylated BU[4] **1** and dodecapropargylated BU[6] **2** were used as clickable platforms to generate architectures decorated with 8 and 12 DNJ inhibitors, respectively. For this purpose, azide-armed N-hexyl DNJ **12**, N-nonyl DNJ **13** and N-nonyl-trivalent DNJ-dendron (tripod) **14** were chosen as peripheral ligands to generate corresponding neoglyco₈BU[4] **3–5** and neoglyco₁₂BU[6] **6–11** derivatives. The syntheses of DNJ-functionalized bambusuril BU[4] **3–5** and the structures of azide DNJ ligands **12–14** are shown in Scheme 1.

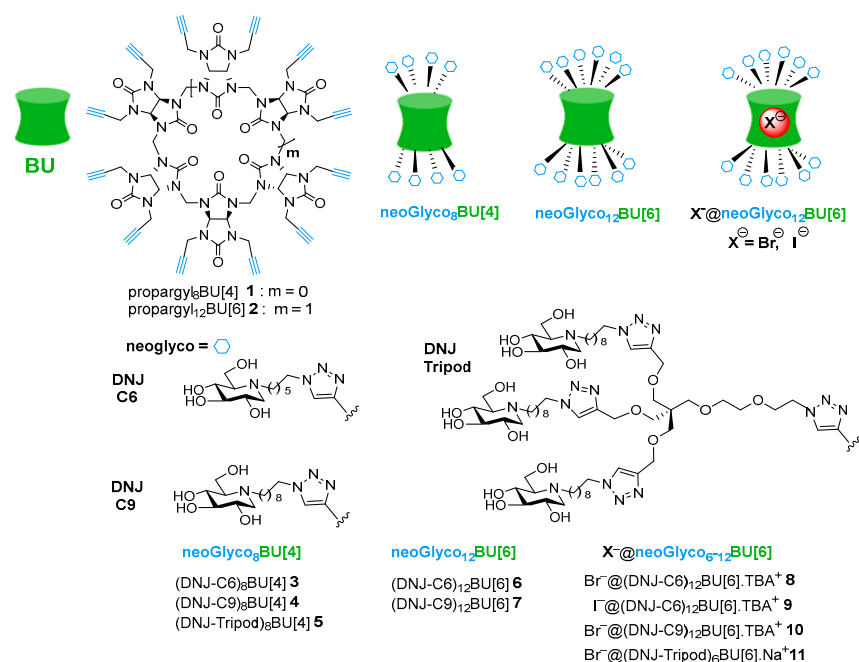
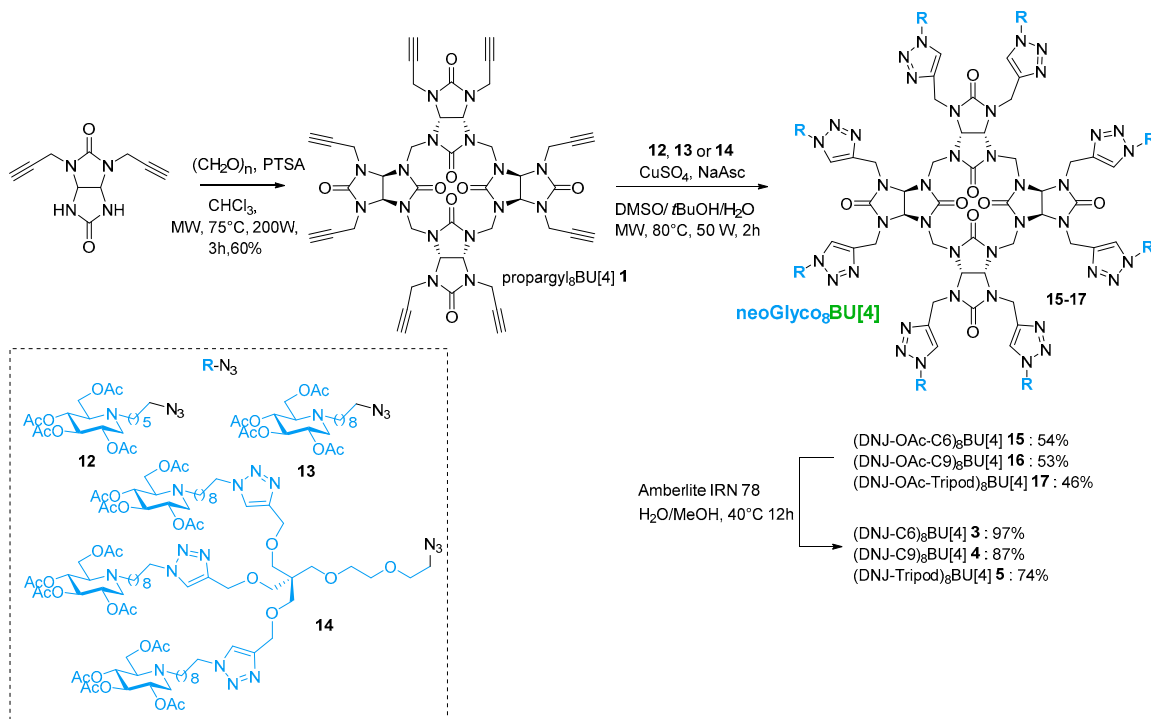


Figure 1. Structures of propargyl₈BU[4] **1**, propargyl₁₂BU[6] **2**, neoglycobambusurils BU[4] **3–5** and BU[6] **6, 7** and $Br^- @ BU[6].TBA^+$ **8, 10–11** and $I^- @ BU[6].TBA^+$ **9** bearing DNJ ligands studied in this paper.

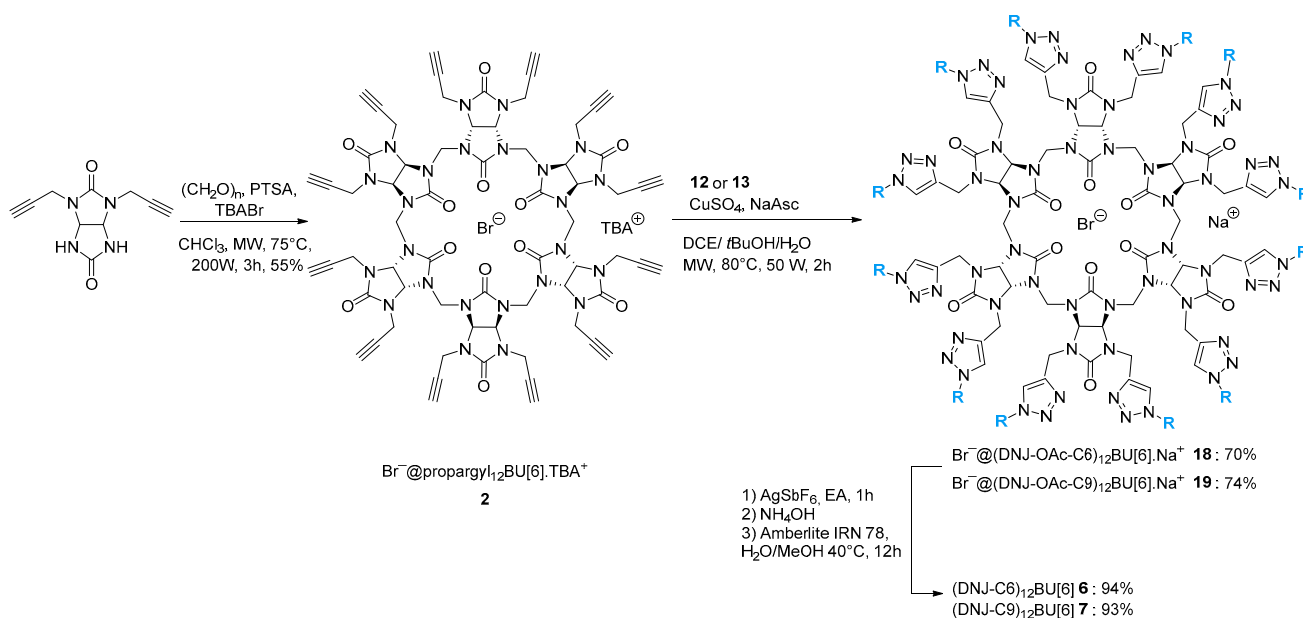


Scheme 1. Synthesis of neoglycobambus[4]urils BU[4] **3, 4** and **5** decorated with C-6, C-9 monovalent DNJ and C-9 trivalent tripod DNJ, respectively.

First, the dipropargylated BU[4] platform **1** was prepared in one step and with 60% yield by condensation of propargylglycoluril and formaldehyde following our reported procedure [14]. Propargyl₈BU[4] **1** was then reacted with peracetylated azido-functionalized C6-DNJ **12** [37,39] through a copper(I)-catalyzed azide alkyne cycloaddition reaction (CuAAC) in the presence of sodium ascorbate in DMSO/*t*BuOH/ H_2O to acquire pro-

tected (DNJ-OAc-C6)₈BU[4] **15** with 54% yield. Use of microwave irradiations shortened the reaction time and increased yield. Subsequently, deacetylation of **15** was set up using anion exchange (OH⁻) amberlite IRN 78 resin as described [37,40] to generate (DNJ-C6)₈BU[4] **3** with 97% yield. Following the same synthetic procedure, (DNJ-OAc-C9)₈BU[4] **16** was isolated with 53% yield from the CuAAC reaction of propargyl₈BU[4] **1** and peracetylated azido-functionalized C9-DNJ **13** [37]. Basic cleavage of OAc groups of **16** afforded (DNJ-C9)₈BU[4] **4** decorated with 8 DNJ (C-9 linker) with 87% yield. Grafting of 24 DNJ derivatives was made possible by the click coupling of protected azido trivalent-C9-DNJ dendron **14** [38,41] on BU[4] **1** to give (DNJ-OAc-Tripod)₈BU[4] **17** with 46% yield. Basic treatment of **17** generated (DNJ-Tripod)₈BU[4] **5** with 74% yield.

A larger platform, Br⁻@propargyl₁₂BU[6].TBA⁺ **2**, that was able to be decorated with 12 iminosugar inhitopes was then submitted to azide-armed DNJ derivatives **12** and **13** to generate, after decomplexation and deprotection steps, the corresponding 12-valent clusters (DNJ-C6)₁₂BU[6] **6** and (DNJ-C9)₁₂BU[6] **7**, respectively (Scheme 2).

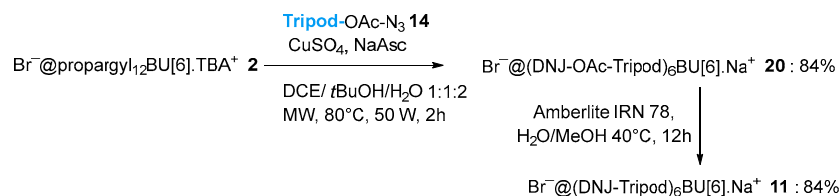


Scheme 2. Synthesis of neoglyco₁₂BU[6] **6**, **7** bearing 12 (C-6, C-9) monovalent DNJ ligands.

First, following our reported procedure, condensation of dipropargyl glycoluril with formaldehyde and TBABr as template promoted the formation of Br⁻@propargyl₁₂BU[6].TBA⁺ **2** with 55% yield [14]. A subsequent CuAAC reaction of **2** with azide-armed DNJ **12** (C6 linker) afforded fully functionalized Br⁻@(DNJ-C6-OAc)₁₂BU[6].Na⁺ **18** with 70% yield. Click reaction of BU **2** with azide-armed DNJ **13** (C9 linker) provided 12-valent Br⁻@(DNJ-C9-OAc)₁₂BU[6].Na⁺ **19** with 74% yield. Decomplexation reactions of Br⁻@BU **18** and **19** were then performed with AgSbF₆ [13] to generate the corresponding anion-free 12-valent iminosugars that were directly submitted to basic resin for the final deprotection step, yielding (DNJ-C6)₁₂BU[6] **6** (94% yield) and (DNJ-C9)₁₂BU[6] **7** (93% yield), respectively.

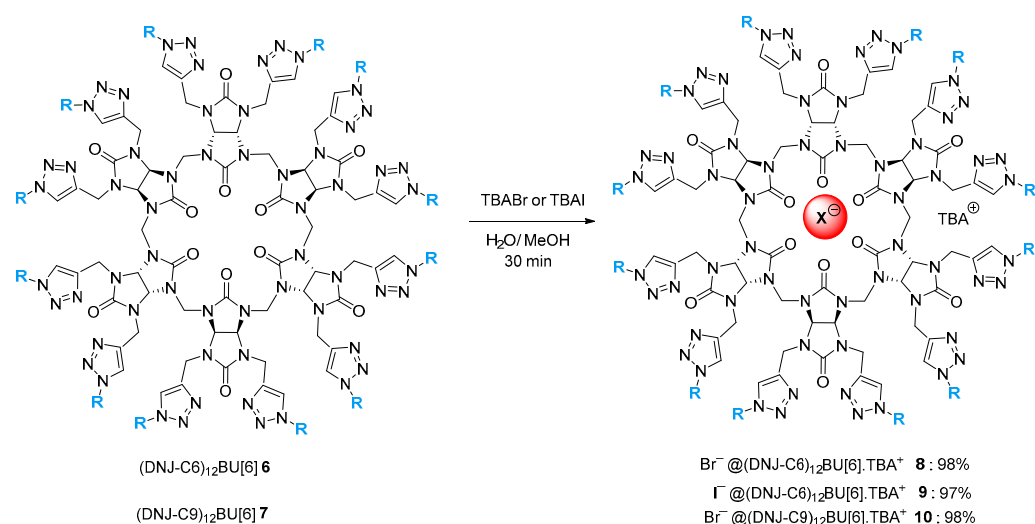
To obtain the 12 × 3-valent DNJ-BU[6] conjugate, Br⁻@propargyl₁₂BU[6].TBA⁺ **2** was reacted with clickable dendron **14** [38] in the presence of CuSO₄ and sodium ascorbate using microwave irradiations to promote full click coupling (Scheme 3). However, using our general click procedure, only partial functionalization of **2** was observed, affording 6 × 3 valent-DNJ-Tripod-BU[6] **20** with 84% yield. Despite many attempts to optimize the reaction conditions (solvent, stoichiometry, microwave power, temperature, reaction time), it was not possible to obtain fully functionalized BU[6]. We hypothesized that the steric hindrance of the DNJ Tripod **14** did not allow the total functionalization of BU[6] **2**. Mass spectra analysis allowed for quantification of the presence of six grafted tripods. The six remaining alkyne functions were observable on the ¹H NMR spectrum of **20**.

Despite its partial functionalization, $\text{Br}^- @(\text{DNJ-Tripod-OAc})_6 \text{BU}[6] \cdot \text{Na}^+$ **20** was submitted to basic resin deprotection to give $\text{Br}^- @(\text{DNJ-Tripod})_6 \text{BU}[6] \cdot \text{Na}^+$ **11** with 84% yield. This interesting cluster bearing 18 DNJ units has been also evaluated as a glycosidase inhibitor.



Scheme 3. Synthesis of $\text{Br}^- @(\text{DNJ-Tripod})_6 \text{BU}[6] \cdot \text{Na}^+$ **11**.

Interestingly, bambusurils BU[6] are known to complex halides, especially iodides, with very high affinity forming a rigid assemblage [1,42]. We hypothesized that such a rigid structure could influence the glycosidase inhibition power of iminosugar–BU conjugates. Towards this goal, TBABr was added to anion-free $(\text{DNJ-C6-OH})_{12} \text{BU}[6]$ **6** in $\text{H}_2\text{O}/\text{MeOH}$ to generate $\text{Br}^- @(\text{DNJ-C6-OH})_{12} \text{BU}[6] \cdot \text{TBA}^+$ **8** (98% yield). Similarly, addition of TBAI to $(\text{DNJ-C6-OH})_{12} \text{BU}[6]$ **6** yielded $\text{I}^- @(\text{DNJ-C9-OH})_{12} \text{BU}[6] \cdot \text{TBA}^+$ **9** (97% yield) and reaction of anion-free $(\text{DNJ-C9-OH})_{12} \text{BU}[6]$ **7** with TBABr gave $\text{Br}^- @(\text{DNJ-C9-OH})_{12} \text{BU}[6] \cdot \text{TBA}^+$ **10** (98% yield). The synthesis of anion@BU[6] **8–10** is reported in Scheme 4.



Scheme 4. Synthesis of $\text{Br}^- @(\text{DNJ-C6})_{12} \text{BU}[6] \cdot \text{TBA}^+$ **8**, $\text{I}^- @(\text{DNJ-C6})_{12} \text{BU}[6] \cdot \text{TBA}^+$ **9** and $\text{Br}^- @(\text{DNJ-C9})_{12} \text{BU}[6] \cdot \text{TBA}^+$ **10**.

The hostguest interaction of anion-free $(\text{DNJ-C6})_{12} \text{BU}[6]$ **6** with iodide anion was evaluated using a direct isothermal titration calorimetry (ITC) method [4,14]. BU[6] **6** bearing 12 DNJ arms (C6 linker) was found to have a good affinity for iodide ($K_a = 4.8 \times 10^5 \text{ M}^{-1}$ in water) (Supplementary Materials Figure S1), similar to our reported results for $(\text{D-glucose})_{12} \text{BU}[6]$ derivatives ($K_a = 2.2 \times 10^5$ and $1.7 \times 10^5 \text{ M}^{-1}$ for iodide complexation in H_2O) [14]. Interestingly, this study shows that C6 linkers, or the nature of the peripheral head (DNJ compared to D-glucose), did not affect complexation. In addition, ITC data clearly indicate that the formation of the iodide complex **9** is driven by enthalpy ($\Delta H = -33, 47 \text{ kJ/mol}$) and that **9** displays a 1:1 stoichiometry in water.

2.2. Glycosidase Inhibition Study

All the new clusters were evaluated against Jack Bean α -mannosidase, a glycosidase highly sensitive to multivalent inhibitor presentation [15–20]. The corresponding inhibition constants are summarized in Table 1. The evaluated DNJ-bambusuril conjugates acted as

competitive inhibitors, with the notable exception of the series of 12-valent clusters with the shorter C6 linker obtained with the BU[6] scaffold which behaved as mixed inhibitors (Table 1, entries 6–8). The inhibition potency of those new clusters was compared to their corresponding monovalent inhibitors, **21** [22] and **22** [37] (Figure 2), to calculate their relative potency (*rp*). Dividing the relative potency by the number of active units gives the relative potency per inhitope (*rp/n*).

Table 1. Inhibition activity of (DNJ)₈BU[4] **3–5** and (DNJ)₁₂BU[6] **6–11** towards Jack Bean α -mannosidase.

Entry	Compound	BU	Alkyl Chain Length	DNJ Units	K_i (μ M)	Inhibition Mode	R_p [a]	rp/n
1	21	-	C6	1	322 [22]	competitive	-	-
2	22	-	C9	1	188 [37]	competitive	-	-
3	3	BU[4]	C6	8	9.7+/-2.9	competitive	33	4
4	4	BU[4]	C9	8	0.71+/-0.55	competitive	265	33
5	5	BU[4]	C9	24	0.024+/-0.004	competitive	7833	326
6	6	BU[6]	C6	12	68.2+/-10.3 147+/-21	mixed	4.7	0.4
7	8	Br ⁻ @BU[6].TBA ⁺	C6	12	85.6+/-10.3 191+/-37	mixed	3.8	0.3
8	9	I ⁻ @BU[6].TBA ⁺	C6	12	108+/-13 162+/-40	mixed	3.0	0.5
9	7	BU[6]	C9	12	1.06+/-0.34	competitive	177	15
10	10	Br ⁻ @BU[6].TBA ⁺	C9	12	0.488+/-0.343	competitive	385	32
11	11	Br ⁻ @BU[6].Na ⁺	C9	18	0.016+/-0.002	competitive	11750	~652

[a] $rp = K_i$ (monovalent reference)/ K_i (neoglycocluster), n = number of inhitope units.



Figure 2. Structure of monovalent inhibitors **21–22**.

As in a previous study with calix[8]arene-based clusters [43], the scaffold has a strong impact on inhibition with the C6 shorter linker. Whereas the inhibitory heads of cluster **3** based on the smaller BU[4] scaffold are individually four times more potent than the reference ($rp/n = 4$), the ones of clusters **6**, **8** and **9** based on BU[6] are less active than the monovalent reference ($rp/n < 1$) and show a different inhibition mode (Table 1 entries 6–8). Noticeably, the inhibition mode and power of the three BU[6] binding bromide or iodide ions (or with a free cavity) are similar, suggesting an overall similar shape. We previously obtained crystals of Cl⁻, Br⁻, I⁻@allyl₁₂BU[6].TBA⁺ [12,13] and of Br⁻, I⁻@propargyl₁₂BU[6].TBA⁺ [14], showing that the halides are included in the cavity and that the geometry of these CH⁺⋯halide bonds are similar, with distances varying with the halogen ionic radius which thus indicates that the macrocycle retains some flexibility [12–14]. Similarly, with C9 linkers, the activities and inhibition mode are not impacted by the presence of anions in the bambusuril cavity (Table 1 entries 9–10). With the longer C9 linker, the impact of the central scaffold, whatever its size, is abolished, giving similar affinity enhancement per DNJ (entries 4, 9 and 10) with C9 enhancement being at least one order of magnitude higher than for the C6 series. This result is in line with previous findings using other scaffolds [15–20,43]. The best results were obtained with clusters **5** and **11** grafted with the trivalent dendron with affinity enhancements one order of magnitude higher than those of compounds **4**, **7** and **10**. The affinity enhancement per inhibitory head of compound **5** is in the same range as for the 24-valent cyclopeptoid bearing the same trivalent dendron [26]. Altogether, those results show that bambusuril scaffolds allow for efficient grafting of glycosidase inhibitors and that

this multimerization induces strong affinity enhancements. Moreover, the fact that activity is not influenced by anion binding opens the way to potential therapeutic applications by inducing accumulation of the encaged anion, and potentially radioactive iodide, in a glycosidase rich environment. It is, for example, well-known that β -glucuronidases are present at high concentration in the microenvironment of most solid tumours [44] and that radioactive iodine is used for the treatment of cancers, including thyroid cancers [45–47].

3. Material and Methods

3.1. General Information and General Experimental Procedures for the Syntheses

Commercially available reagents were used without further purification. All reactions were performed under inert atmosphere using anhydrous solvents which were dried and distilled before being used. Thin-layer chromatograms (TLC) and flash chromatography separations were respectively performed on precoated silica gel 60 F254 plates (0.25 mm) and on Merck Kieselgel 60 (grading 40–63 μ m). Microwave syntheses were conducted using a CEM Focused Microwave Discover[®] SP-X System reactor. The reactions were performed for 2–4 h under magnetic stirring in 10 or 35 mL sealed Discovered SP vessels closed with Activent[®]caps. The dynamic control method was used for all microwave reactions where the temperature and the pressure were set ($P = 50$ W, $T = 80$ °C, PowerMax on). ¹H NMR spectra (400 MHz) and ¹³C NMR spectra (100 MHz) were recorded on a Bruker Avance 400 MHz spectrometer. Chemical shifts and coupling constants are reported in parts per million (ppm) and in Hertz (Hz), respectively. HRMS and electrospray mass spectra (ESIMS) were obtained from an LCT Premier XE using electro spray ionization coupled with a time flight analyzer (ESI-TOF). Infrared spectra (IR) were recorded on a Perkin Elmer UAR Two Spectrum spectrometer. Electrospray mass spectra were obtained using an ESI-Quadripole autopurify Waters (pump: 2545, mass: ZQ2000) mass Spectrometer. Optical rotations were measured on a JASCO P-2000 Polarimeter. Melting points were measured on a Büchi Melting point B540.

3.1.1. General Procedure A for CuAAC Reaction of Propargyl₈BU[4]

To a solution of octapropargyl bambus[4]uril **1** (10 to 15 mg, 1 eq.) and azide ligand (9 eq.) in DMF/H₂O (0.6 mL, 5/1) in a microwave reactor, a solution of sodium ascorbate 1 M in water (0.4 eq.) and a solution of CuSO₄ 5H₂O 1M in H₂O (0.8 eq.) were added. The reaction was subjected to microwave irradiations under magnetic stirring from 30 min to 4 h at 80 °C. A solution of CH₃CN/H₂O/30w% NH₄OH (16 mL, 15/0.5/0.5, *v/v/v*) was then added to the crude and the mixture was filtered on a small pad of SiO₂ and eluted with a solution of CH₃CN/H₂O/30w%-NH₄OH (15:0.5:0.5, *v/v/v*). The filtrate was concentrated under vacuum and purified by flash silica gel chromatography (SiO₂; CH₂Cl₂/MeOH, 99:1 to 95:5) to afford the corresponding 8-clicked iminosugars BU[4].

3.1.2. General Procedure B for CuAAC Reaction of Propargyl₁₂BU[6]

To a solution of dodecapropargylbambus[6]uril *tetra*-butyl bromide **2** (10 to 15 mg, 1 eq.) and azide ligand (16 eq.) in DCE/H₂O/*t*BuOH (0.5/1/1.2 mL) in a microwave reactor, a solution of sodium ascorbate 1 M in water (4 eq.) and a solution of CuSO₄.5H₂O 1M in H₂O (2 eq.) were added. The reaction was subjected to microwave irradiations under magnetic stirring for 2 h at 80 °C. The mixture was then concentrated under vacuum and diluted with CH₃CN/H₂O/30w% NH₄OH (9/1/1, 11 mL). The mixture was filtered on a small pad of SiO₂ (typically 1 cm thick) that was washed with this same eluent, CH₃CN/H₂O/30w%-NH₄OH (9/1/1, 25 mL). The filtrate was concentrated under vacuum and purified by flash silica gel chromatography (SiO₂; CH₂Cl₂/MeOH, 99:1 to 90) to afford the corresponding 12-clicked iminosugars BU[6].

3.1.3. General Procedure C for Deacetylation of Sugars

Amberlite IRN 78 (HO⁻) (n g/mmol with n = number of OAc) was added to a solution of acetylated-iminosugars bambusuril (1 eq.) in H₂O/MeOH (1/1, 600 μ L). The suspension

was stirred from 4 h to 12 h at 40 °C. The resin was removed by filtration and washed with methanol and water. The filtrate was concentrated under vacuum to give BU-iminosugars.

3.1.4. Synthesis (DNJ-OAc-C6)₈BU[4] 15

Following general procedure A and starting with propargyl₈bambus[4]uril **1** (10.1 mg, 10.9 μmol, 1 eq.) and azidoiminosugar **12** (60 mg, 132 μmol, 12 eq.), (DNJ-OAc-C6)₈BU[4] **15** (27.1 mg, 54% yield) was obtained as a colorless oil. ¹H NMR (300 MHz, CDCl₃): δ (ppm) 7.56 (s, 8H, H13), 5.74 (s, 6H, H17), 5.10–4.99 (m, 16H, H3, H4), 4.99–4.89 (m, 8H, H2), 4.66–4.44 (m, 24H, H15, H19), 4.42–4.21 (m, 16H, H12), 4.20–4.04 (m, 16H, H6), 3.17 (dd, *J* = 11.0, 5.0 Hz, 8H, H1a), 2.78–2.66 (m, 8H, H7a), 2.66–2.58 (m, 8H, H5), 2.58–2.47 (m, 8H, H7b), 2.29 (dd, *J* = 11.0, 10.5 Hz, 8H, H1b), 2.10–1.96 (singlets, 96H, CH₃-C=O), 1.93–1.81 (m, 16H, H11), 1.53–1.08 (m, 48H, H8, H9, H10); ¹³C NMR (75 MHz, CDCl₃): δ (ppm) 170.9, 170.4, 170.1, 169.8 (CH₃-C=O), 159.7, 158.3 (C16, C18), 143.8 (C14), 122.8 (C13), 74.8 (C3), 71.6 (C17), 69.6 (C4), 69.5 (C2), 61.7 (C5), 59.7 (C6), 53.0 (C1), 51.7 (C7), 50.4 (C12), 39.0 (C15), 30.3 (C11), 26.8, 26.6 (C9, C10), 25.0 (C8), 21.0, 20.85, 20.8 (CH₃-C=O), C-9 could not be observed with 1024 scans; IR (neat, ν_{max}/cm⁻¹) 1744 (CH₃-C=O), 1710 (NC=O); HRMS (ESI⁺): *m/z* calcd for C₂₀₄H₂₉₇N₄₈Na₂O₇₂ [M + H + 2Na]³⁺: 1539.0278, found 1539.0257; [α]_D²⁰ = +2.2 (c 1, CH₃OH).

3.1.5. Synthesis of (DNJ-OAc-C9)₈BU[4] 16

Following general procedure A and starting with propargyl₈bambus[4]uril **1** (10 mg, 10.9 μmol, 1 eq.) and azidoiminosugar **13** (65 mg, 130 μmol, 12 eq.), (DNJ-OAc-C9)₈BU[4] **16** (28.3 mg, 53% yield) was isolated as a colorless oil. ¹H NMR (400 MHz, CDCl₃): δ (ppm) 7.55 (br s, 8H, H16), 5.74 (br s, 6H, H20), 5.10–4.99 (m, 16H, H3, H4), 4.95–4.90 (m, 8H, H2), 4.65–4.51 (m, 24H, H18, H22), 4.38–4.23 (m, 16H, H15), 4.19–4.09 (m, 16H, H6), 3.18 (dd, *J* = 11.2, 4.9 Hz, 8H, H1a), 2.76–2.66 (m, 8H, H7a), 2.65–2.60 (m, 8H, H5), 2.59–2.50 (m, 8H, H7b), 2.32 (dd, *J* = 11.2, 10.3 Hz, 8H, H1b), 2.07 (s, 24H, CH₃-C=O), 2.0–1.97 (singlets, 72H, CH₃-C=O), 1.89–1.83 (m, 16H, H14), 1.50–1.11 (m, 96H, H8, H9, H10, H11, H12, H13); ¹³C NMR (100 MHz, CDCl₃): δ (ppm) 171.0, 170.5, 170.1, 169.8 (CH₃-C=O), 159.7, 158.4 (C-19, C-21), 143.8 (C-17), 122.7 (C-16), 74.8 (C-3), 71.5 (C-20), 69.7 (C-4), 69.6 (C-2), 61.6 (C-5), 59.7 (C-6), 53.0 (C-1), 51.9 (C-7), 50.6 (C-15), 38.9 (C-18), 30.3 (C-14), 29.8, 29.6, 29.1, 27.3, 26.7 (C-9, C-10, C-11, C-12, C-13), 24.8 (C-8), 21.0, 20.97, 20.88, 20.81 (CH₃-C=O), C22 could not be observed with 1024 scans; IR (neat, ν_{max}/cm⁻¹) 1742 (CH₃-C=O), 1705 (NC=O); HRMS (ESI): *m/z* calcd for C₂₂₈H₃₄₇N₄₈O₇₂ [M + 3H]³⁺: 1636.4983, found 1636.5006; [α]_D²⁰ = +2.6 (c 1, CH₃OH).

3.1.6. Synthesis of (DNJ-OAc-Tripod)₈BU[4] 17

Following general procedure A and starting with propargyl₈bambus[4]uril **1** (3 mg, 3.3 μmol, 1 eq.) and azido-tripod **14** (84 mg, 45.6 μmol, 14 eq.), (DNJ-OAc-tripod)₈BU[4] **16** (23.7 mg, 1.5 μmol, 46% yield) was isolated as a colorless oil. ¹H NMR (400 MHz, CDCl₃): δ (ppm) 7.69–7.67 (br s, 8H, H26), 7.65–7.52 (br s, 24H, H16), 5.76 (br s, 6H, H30), 5.11–4.99 (m, 48H, H3, H4), 4.99–4.90 (m, 24H, H2), 4.60–4.44 (m, 88H, H18, H25, H28, H32), 4.31 (t, *J* = 7.4 Hz, 48H, H15), 4.17–4.11 (br s, 48H, H6), 3.88–3.75 (m, 16H, H24), 3.62–3.35 (m, 96H, H19, H21, H22, H23), 3.18 (dd, *J* = 11.2, 5.1 Hz, 24H, H1a), 2.76–2.66 (m, 24H, H7a), 2.66–2.60 (m, 24H, H5), 2.60–2.48 (m, 24H, H7b), 2.32 (dd, *J* = 11.2, 10.5 Hz, 24H, H1b), 2.07–1.98 (several singlets, 288H, CH₃-C=O), 1.93–1.82 (m, 48H, H14), 1.48–1.12 (m, 288H, H8, H9, H10, H11, H12, H13); ¹³C NMR (CDCl₃, 100 MHz): δ (ppm) 171.0, 170.5, 170.1, 169.9 (CH₃-C=O), 159.8, 158.4 (C29, C31), 145.3 (C27), 143.7 (C17), 123.9 (C26), 122.7 (C16), 74.8 (C3), 71.0, 70.3, 70.0 (C21, C22, C23), 69.6 (C4, C24), 69.5 (C2), 69.3 (C19), 65.1 (C18), 61.5 (C5), 59.6 (C6), 53.0 (C1), 51.9 (C7), 50.4 (C15, C25), 45.5 (C20), 38.7 (C28), 30.5 (C14), 29.8, 29.6, 29.1, 27.3, 26.7 (C9, C10, C11, C12, C13), 24.7 (C8), 21.01, 20.98, 20.88, 20.8 (CH₃-C=O); IR (neat, ν_{max}/cm⁻¹) 1743 (strong, (CH₃-C=O)); HRMS (ESI, deconvoluted): *m/z* calcd for C₇₄₀H₁₁₆₄N₁₃₆O₂₄₀ [M + 12H]¹²⁺: 1317.15, found 1317.16; [α]_D²⁰ = +1.4 (c 1, CH₃OH).

3.1.7. Synthesis of (DNJ-C6)₈BU[4] **3**

Following general procedure C and starting with (DNJ-OAc-C6-triazol)₈BU[4] **15** (27.4 mg, 6.0 μmol), corresponding (DNJ-C6-triazol)₈BU[4] **3** (18.8 mg, 5.8 μmol, 97% yield) was obtained as a colorless oil. ¹H NMR (400 MHz, D₂O): δ (ppm) 7.91 (br s, 8H, H13), 5.81 (br s, 6H, H17), 4.70–4.58 (m, 16H, H15), 4.53–4.39 (m, 8H, H19), 4.40–4.22 (m, 16H, H12), 3.87–3.77 (m, 16H, H6), 3.53 (td, *J* = 10.0 and 4.8 Hz, 8H, H2), 3.40–3.34 (m, 8H, H4), 3.26–3.21 (m, 8H, H3), 2.96 (dd, *J* = 10.3, 4.8 Hz, 8H, H1a), 2.75–2.60 (m, 8H, H7a), 2.60–2.48 (m, 8H, H7b), 2.29–2.14 (m, 16H, H1b, H5), 1.87–1.71 (m, 16H, H11), 1.45–1.31 (m, 16H, H8), 1.27–1.10 (m, 32H, H9, H10); ¹³C NMR (100 MHz, D₂O): δ (ppm) 160.0, 159.3 (H16, H18), 143.1 (H14), 123.9 (H13), 78.4 (H3), 71.3 (H17), 70.0 (H4), 68.8 (H2), 65.1 (H5), 57.5 (H6), 55.4 (H1), 51.9 (H7), 50.3 (H12), 48.5 (C19), 38.3 (C15), 29.4 (C11), 26.2, 25.5 (C9, C10), 22.6 (C8); IR (neat, ν_{max}/cm⁻¹) 1694 (strong, NC=O); HRMS (ESI): *m/z* calcd for C₁₄₀H₂₃₅N₄₈O₄₀ [M + 3H]³⁺: 1076.2605, found 1076.2629; [α]_D²⁰ = −12.3 (c 1, H₂O + TFA (1 drop)).

3.1.8. Synthesis of (DNJ-C9)₈BU[4] **4**

Following general procedure C and starting with (DNJ-OAc-C9)₈BU[4] **16** (23.5 mg, 4.8 μmol), corresponding (DNJ-C9)₈BU[4] **4** (14.9 mg, 4.2 μmol, 87%) was obtained as a colorless oil. ¹H NMR (400 MHz, MeOD): δ (ppm) 7.89 (br s, 8H, H16), 5.80 (br s, 6H, H20), 4.66–4.60 (br s, 16H, H18), 4.59–4.53 (br s, 8H, H22), 4.38 (t ap, *J* = 6.9 Hz, 16H, H15), 3.86–3.82 (m, 16H, H6), 3.47 (td, *J* = 9.4, 4.6 Hz, 8H, H2), 3.40–3.35 (m, 8H, H4), 3.13 (dd, *J* = 9.0 Hz, 8H, H3), 2.98 (dd, *J* = 11.7, 5.0 Hz, 8H, H1a), 2.83–2.71 (m, 8H, H7a), 2.62–2.49 (m, 8H, H7b), 2.16 (dd, *J* = 11.1 Hz, 8H, H1b), 2.10 (d, *J* = 9.1 Hz, 8H, H5), 1.93–1.84 (m, 16H, H14), 1.53–1.42 (m, 16H, H8), 1.39–1.21 (m, 80H, H9, H10, H11, H12, H13); ¹³C NMR (125 MHz, MeOD, 2218 scans, cryogenic probe): δ (ppm) 161.3, 160.1 (C19, C21), 144.7 (C17), 124.7 (C16), 80.4 (C3), 72.6 (C20), 71.9 (C4), 70.6 (C2), 67.2 (C5), 59.4 (C6), 57.6 (C1), 53.7 (C7), 51.7 (C22), 51.5 (C15), 39.6 (C18), 31.3 (C14), 30.5, 30.1, 30.0, 28.6, 27.5 (C9, C10, C11, C12, C13), 24.9 (C8); IR (neat, ν_{max}/cm⁻¹) 3343 (strong broad, OH), 1696 (strong, NC=O); HRMS (ESI, deconvoluted): *m/z* calcd for C₁₆₄H₂₈₇N₄₈O₄₀ [M + 7H]⁷⁺: 509.8837, found 509.8893; *m/z* calcd for C₁₆₄H₂₈₆N₄₈O₄₀ [M + 6H]⁶⁺: 594.6964, found 594.6979; *m/z* calcd for C₁₆₄H₂₈₅N₄₈O₄₀ [M + 5H]⁵⁺: 713.4341, found 713.4314; [α]_D²⁰ = −7.1 (c 1, CH₃OH/H₂O 94/6).

3.1.9. Synthesis of (DNJ-Tripod)₈BU[4] **5**

Following general procedure C and starting with (DNJ-OAc-tripod)₈BU[4] **17** (23.5 mg, 1.5 μmol), corresponding (DNJ-tripod)₈BU[4] **7** (12.9 mg, 1.1 μmol, 74% yield) was obtained as a colorless oil. ¹H NMR (400 MHz, MeOD): δ (ppm) 8.03–7.92 (br s, 32H, H16, H26), 5.88–5.72 (br s, 6H, H30), 4.60–4.44 (m, 80H, H18, H25, H28), 4.42–4.27 (m, 56H, H15, H32), 3.93–3.76 (m, 64H, H6, H24), 3.56–3.33 (m, 144H, H2, H4, H19, H21, H22, H23), 3.19 (t, *J* = 9.2 Hz, 24H, H3), 2.97 (dd, *J* = 11.1, 4.9 Hz, 24H, H1a), 2.78–2.66 (m, 24H, H7a), 2.64–2.52 (m, 24H, H7b), 2.21 (t, *J* = 10.8 Hz, 24H, H1b), 2.15 (dt, *J* = 9.4, 2.6 Hz, 24H, H5), 1.88–1.76 (m, 48H, H14), 1.49–1.37 (m, 48H, H8), 1.31–1.15 (m, 240H, H9, H10, H11, H12, H13); ¹³C NMR (125 MHz, MeOD, 12288 scans): δ (ppm) 170.9, 170.0 (C29, C31), 146.1 (C17, C27), 125.2 (C16, C26), 80.4 (C3), 71.9 (C4), 70.6 (C2), 73.1, 72.5, 72.1, 71.3, 70.4, 70.1, 69.5 (C19, C21, C22, C23, C24, C30), 67.1 (C5), 65.4 (C18), 59.5 (C6), 57.5 (C1), 53.8 (C7), 51.5 (C15, C25), 50.7 (C32), 46.5 (C20), 40.1 (C28), 31.3 (C14), 30.6, 30.1, 28.6, 27.5 (C9, C10, C11, C12, C13), 24.9 (C8); IR (neat, ν_{max}/cm⁻¹) 3359 (strong broad, OH), 1703 (strong, NC=O); HRMS (ESI, deconvoluted): *m/z* calcd for C₅₄₈H₉₇₀N₁₃₆O₁₄₄ [M + 10H]¹⁰⁺: 1176.8321, found 1176.8032; [α]_D²⁰ = −4.7 (c 0.8, CH₃OH).

3.1.10. Synthesis of Br⁻@(DNJ-OAc-C6)₁₂BU[6].Na⁺ **18**

According to procedure B and starting with propargyl₁₂bambus[6]uril **2** (8.4 mg, 4.90 μmol, 1 eq.) and azidoiminosugar **12** (35.9 mg, 78.60 μmol, 16 eq.), sodium ascorbate (19.7 μL, 19.70 μmol, 4 eq.) and copper sulfate (9.8 μL, 9.80 μmol, 2 eq.) were added. After purification, Br⁻@(DNJ-OAc-C6)₁₂BU[6].Na⁺ **18** was obtained (23.8 mg, 70% yield). ¹H

NMR (400 MHz, CDCl₃): δ (ppm) 7.49 (s, 12H, H13), 5.79 (s, 12H, H17), 5.06–4.93 (m, 60H, H2, H3, H4, H15), 4.66–4.58 (br s, 12H, H19), 4.20–4.14 (m, 48H, H6, H12), 3.18–3.16 (m, 12H, H1'a), 2.63–2.61 (m, 12H, H7a), 2.60–2.52 (m, 12H, H5), 2.51–2.49 (m, 12H, H7b), 2.28 (t, $J = 10.8$ Hz, 12H, H1b), 2.05–2.02–2.01–2.00 (s, 144H, CH₃-C=O), 1.85–1.82 (br s, 24H, H11), 1.39–1.24 (m, 72H, H8, H9, H10); ¹³C NMR (100 MHz, CDCl₃): δ (ppm) 170.9–170.4–170.1–169.8 (CH₃-C=O), 159.0 (C16, C18), 145.6 (C14), 122.8 (C13), 74.6 (C4), 69.3 (C17), 69.1 (C3), 61.7 (C5), 59.5 (C6), 53.6 (C1), 52.8 (C7), 51.9 (C12), 50.4 (C2), 47.6 (C19), 39.4 (C15), 30.2 (C11), 26.7 (C9), 26.6 (C10), 24.7 (C8), 21.0, 20.9, 20.8 (CH₃-C=O); IR (neat, $\nu_{\max}/\text{cm}^{-1}$) 2939 (CH₂), 1742 (CH₃-C=O), 1703 (NC=O), 1478 (CH₂), 1218 (C-N); HRMS (ESI+): m/z calculated for [C₃₀₆H₄₄₄N₇₂O₁₀₈+6H⁺]⁶⁺: 1143.5317, found 1143.5304; $[\alpha]_{\text{D}}^{20} = 7.2$ (c 0.18, CHCl₃).

3.1.11. Synthesis of Br⁻@(DNJ-OAc-C9)₁₂BU[6] Na⁺ **19**

According to procedure B, propargyl₁₂bambus[6]uril **2** (7.9 mg, 4.60 μmol , 1 eq.), azidoiminosugar **13** (36.8 mg, 73.80 μmol , 16 eq.), sodium ascorbate (18.4 μL , 18.40 μmol , 4 eq.) and copper sulfate (9.2 μL , 9.20 μmol , 2 eq.) were added. After purification, Br⁻@(DNJ-OAc-C9)₁₂BU[6].Na⁺ **19** was obtained (25.1 mg, 74%). ¹H NMR (400 MHz, CDCl₃): δ (ppm) = 7.46 (br s, 12H, H16), 5.78 (br s, 12H, H20), 5.06–4.94 (m, 48H, H2, H3, H4, H22), 4.62 (br s, 24H, H18), 4.18–4.13 (m, 48H, H6, H15), 3.17 (dd, $J = 11.4, 5.0$ Hz, 12H, H1a), 2.74–2.68 (m, 12H, H7a), 2.63–2.58 (m, 12H, H5), 2.57–2.52 (m, 12H, H7b), 2.31 (t, $J = 11.0$ Hz, 12H, H1b), 2.06, 2.01, 2.01, 1.99 (s, 144H, CH₃-C=O), 1.84–1.74 (m, 24H, H14), 1.37–1.23 (m, 144H, H8, H9, H10, H11, H12, H13); ¹³C NMR (100 MHz, CDCl₃): δ (ppm) = 171.0, 170.5, 170.1, 169.9 (CH₃-C=O), 160.6, 159.0 (C19, C21), 145.4 (C17), 122.2 (C16), 74.8 (C4), 69.5 (C2, C3, C20), 61.5 (C5), 59.6 (C6), 53.0 (C1), 51.9 (C7), 50.4 (C15), 47.8 (C22), 39.1 (C18), 30.3 (C14), 29.6, 29.1, 27.3, 26.8 (C9, C10, C11, C12, C13), 24.7 (C8), 21.0, 20.9, 20.8, 20.7 (CH₃-C=O); IR (neat, $\nu_{\max}/\text{cm}^{-1}$) 2930 (CH₂), 1743 (CH₃-C=O), 1704 (NC=O), 1478 (CH₂), 1225 (C-N), 1032 (C-O); HRMS (ESI+): m/z calculated for [C₃₄₂H₅₁₆N₇₂O₁₀₈+7H⁺]⁷⁺: 1052.3944, found 1052.3943; $[\alpha]_{\text{D}}^{20} = 6.0$ (c 0.24, CHCl₃).

3.1.12. Synthesis of (DNJ-C6)₁₂BU[6] **6**

To a solution of Br⁻@(DNJ-OAc-C6)₁₂BU[6].Na⁺ **18** (18.8 mg, 2.7 μmol , 1 eq.) in EtOAc (2 mL), AgSbF₆ (1.6 mg, 5.4 μmol , 2 eq.) was added and the mixture was sonicated at 25 °C for 1 h to generate a white precipitate of AgBr. NH₄OH (2 mL, 30% aqueous solution) was then added and the organic solution was separated, washed with water (2 \times 2 mL) and concentrated under vacuum to give corresponding anion-free BU that was directly solubilized in H₂O/MeOH (1/1, 2 mL). Amberlite IRN 78 (HO⁻) (125 mg) was added and the suspension was heated for 12 h at 40 °C. The mixture was diluted with MeOH (1 mL) and the resin was removed by filtration before being washed with H₂O (1 mL) and MeOH (1 mL). The filtrate was concentrated under vacuum to afford anion-free (DNJ-C6)₁₂BU[6] **6** (12.2 mg, 94% yield). ¹H NMR (400 MHz, D₂O): δ (ppm) = 7.93 (br s, 12H, H13), 5.73 (br s, 12H, H17), 4.67–4.35 (m, 36H, H15, H19), 4.34–4.13 (m, 24H, H12), 3.89–3.77 (m, 24H, H6), 3.53 (td, $J = 10.2, 5.0$ Hz, 12H, H2), 3.38 (t, $J = 9.6$ Hz, 12H, H3), 3.25 (t, $J = 9.4$ Hz, 12H, H4), 2.97 (dd, $J = 11.1, 4.6$ Hz, 12H, H1a), 2.75–2.61 (m, 12H, H7a), 2.59–2.47 (m, 12H, H7a), 2.28–2.17 (m, 24H, H1b, H5), 1.86–1.72 (m, 24H, H11), 1.43–1.31 (m, 24H, H8), 1.23–1.12 (m, 48H, H9, H10); ¹³C NMR (100 MHz, D₂O): δ (ppm) = 159.8, 158.8 (C16, C18), 144.4 (C14), 123.3 (C13), 78.3 (C4), 69.9 (C17), 68.8 (C3), 68.5 (C2), 64.9 (C5), 57.4 (C6), 55.4 (C1), 51.8 (C7), 50.3 (C12), 49.2 (C19), 38.9 (C15), 29.3 (C11), 26.1 (C9), 25.5 (C10), 22.6 (C8); IR (neat, $\nu_{\max}/\text{cm}^{-1}$) 3337 (OH), 2923 (CH₂), 1703 (NC=O), 1484 (CH₂), 1216 (C-N), 1064 (C-O); HRMS (ESI+): m/z calculated for [C₂₁₀H₃₄₈N₇₂O₆₀+6H⁺]⁶⁺: 807.4472, found 807.4462; $[\alpha]_{\text{D}}^{20} = 1.7$ (c 0.16, H₂O).

3.1.13. Synthesis of (DNJ-C9)₁₂BU[6] **7**

To a solution of (DNJ-OAc-C9)₁₂BU[6] **19** (23.4 mg, 3.1 μmol , 1 eq.) in EtOAc (2 mL), AgSbF₆ (1.83 mg, 6.3 μmol , 2 eq.) was added and the mixture was sonicated at 25 °C for

1 h to generate a white precipitate of AgBr. NH_4OH (2×1 mL, 30% aqueous solution) was then added and the organic solution was separated, washed with water (2×1 mL) and concentrated under vacuum to give corresponding anion-free BU that was solubilized in $\text{H}_2\text{O}/\text{MeOH}$ (1/1, 2 mL). Amberlite IRN 78 (HO^-) (135 mg) was added and the suspension was heated for 12 h at 40°C . The mixture was diluted with MeOH (1 mL) and the resin was removed by filtration and washed with H_2O (1 mL) and MeOH (1 mL). The filtrate was concentrated under vacuum to afford anion-free (DNJ-C9)₁₂BU[6] **7** (15.6 mg, 93% yield). ^1H NMR (400 MHz, $\text{D}_2\text{O}/\text{MeOD}$ 0.3/0.2): δ (ppm) = 7.84 (br s, 12H, H16), 5.72 (br s, 12H, H20), 4.63–4.29 (m, 36H, H18, H22), 4.26–4.16 (m, 24H, H15), 3.83–3.78 (m, 24H, H6), 3.52–3.48 (m, 12H, H4), 3.37–3.31 (m, 12H, H2), 3.22–3.18 (m, 12H, H3), 2.95 (d, $J = 6.3$ Hz, 12H, H1a), 2.70–2.59 (m, 12H, H7a), 2.58–2.48 (m, 12H, H7b), 2.24–2.14 (m, 24H, H1b, H5), 1.78–1.72 (m, 24H, H14), 1.42–1.35 (m, 24H, H8), 1.24–0.95 (m, 120H, H9, H10, H11, H12, H13); ^{13}C NMR (150 MHz, $\text{D}_2\text{O}/\text{MeOD}$ 0.3/0.2): δ (ppm) = 161.3, 160.3 (C19–C21), 146.2 (C17), 124.8 (C16), 79.9 (C4), 71.4 (C20), 70.2 (C2, C3), 66.8 (C5), 58.9 (C6), 57.0 (C1), 53.9 (C7), 51.8 (C22), 40.5 (C15, C18), 31.2 (C14), 30.5, 30.0, 28.5, 27.5 (C9, C10, C11, C12, C13), 24.5 (C8); IR (neat, $\nu_{\text{max}}/\text{cm}^{-1}$) 3370 (OH), 2926 (CH_2), 1708 (NC=O), 1472 (CH_2), 1215 (C-N), 1046 (C-O); HRMS (ESI+): m/z calculated for $[\text{C}_{246}\text{H}_{420}\text{N}_{72}\text{O}_{60}+9\text{H}^+]^{9+}$: 594.6965, found 594.6973; $[\alpha]_{\text{D}}^{20} = 5.9$ ($c = 0.18$ $\text{H}_2\text{O}/\text{MeOH}$ 3/7).

3.1.14. Synthesis of $\text{Br}^-@(\text{DNJ-C6})_{12}\text{BU}[6].\text{TBA}^+$ **8**

To a solution of (DNJ-C6)₁₂BU[6] **6** (9.1 mg, 1.88 μmol , 1 eq.) in 0.5 mL of H_2O , a solution of TBABr in H_2O (64.1 μL , $c = 29.3$ $\mu\text{M}/\text{mL}$, 1 eq.) was added. The mixture was sonicated for 30 min and was lyophilized to afford $\text{Br}^-@(\text{DNJ-C6})_{12}\text{BU}[6].\text{TBA}^+$ **8** (9.5 mg, 98% yield). ^1H NMR (400 MHz, D_2O): δ (ppm) = 7.93 (br s, 12H, H13), 5.81 (br s, 12H, H17), 4.72–4.53 (m, 36H, H15, H19), 4.32–4.28 (m, 24H, H12), 3.82–3.78 (m, 24H, H6), 3.58–3.47 (m, 12H, H2), 3.37 (t, $J = 9.5$ Hz, 12H, H3), 3.29–3.24 (m, 12H, H4), 3.24–3.15 (8H, m, N-($\text{CH}_2\text{-CH}_2\text{-CH}_2\text{-CH}_3$)₄), 2.98–2.93 (m, 12H, H1a), 2.74–2.63 (m, 12H, H7a), 2.52–2.41 (m, 12H, H7b), 2.32–2.18 (m, 32H, H1b, H5, N-($\text{CH}_2\text{-CH}_2\text{-CH}_2\text{-CH}_3$)₄), 1.91–1.78 (m, 24H, H11), 1.68–1.59 (m, 8H, N-($\text{CH}_2\text{-CH}_2\text{-CH}_2\text{-CH}_3$)₄), 1.38–1.16 (m, 72H, H8, H9, H10), 0.94 (t, $J = 7.3$ Hz, 12H, N-($\text{CH}_2\text{-CH}_2\text{-CH}_2\text{-CH}_3$)₄); ^{13}C NMR (100 MHz, D_2O): δ (ppm) = 160.3, 159.6 (C16, C18), 145.3 (C14), 123.9 (C13), 78.9 (C4), 70.5 (C17), 69.4 (C3), 65.7 (C2), 58.7 (N- $\text{CH}_2\text{-CH}_2\text{-CH}_2\text{-CH}_3$), 57.9 (C5), 55.9 (C6), 52.5 (C1), 50.9 (C7), 48.1 (C12, C19), 39.8 (C15), 29.9 (N- $\text{CH}_2\text{-CH}_2\text{-CH}_2\text{-CH}_3$), 26.8 (C11), 26.2 (C9), 23.8 (C10), 23.3 (C8), 19.8 (N- $\text{CH}_2\text{-CH}_2\text{-CH}_2\text{-CH}_3$), 13.4 (N- $\text{CH}_2\text{-CH}_2\text{-CH}_2\text{-CH}_3$); IR (neat, $\nu_{\text{max}}/\text{cm}^{-1}$) 3374 (OH), 2928 (CH_2), 1701 (NC=O), 1481 (CH_2), 1215 (C-N), 1055 (C-O); $[\alpha]_{\text{D}}^{20} = +3.5$ (c 0.14, H_2O).

3.1.15. Synthesis of $\text{I}^-@(\text{DNJ-C6})_{12}\text{BU}[6].\text{TBA}^+$ **9**

To a solution of (DNJ-C6)₁₂BU[6] **6** (8.5 mg, 1.75 μmol , 1 eq.) in 0.5 mL of H_2O was added a solution of TBAI in H_2O (65.9 μL , $c = 26.5$ $\mu\text{M}/\text{mL}$, 1 eq.). The reaction mixture was sonicated for 30 min and then lyophilized to afford $\text{I}^-@(\text{DNJ-C6})_{12}\text{BU}[6].\text{TBA}^+$ **9** (8.8 mg, 97% yield). ^1H NMR (400 MHz, D_2O): δ (ppm) = 7.93 (br s, 12H, H13), 5.98 (br s, 12H, H17), 4.72–4.53 (m, 36H, H15, H19), 4.38–4.29 (m, 24H, H12), 3.83–3.80 (m, 24H, H6), 3.57–3.48 (m, 12H, H2), 3.37 (t, $J = 9.6$ Hz, 12H, H3), 3.28–3.21 (m, 20H, H4, N-($\text{CH}_2\text{-CH}_2\text{-CH}_2\text{-CH}_3$)₄), 3.01–2.95 (m, 12H, H1a), 2.70–2.59 (m, 12H, H7a), 2.58–2.49 (m, 12H, H7b), 2.25–2.18 (m, 32H, H1b, H5, N-($\text{CH}_2\text{-CH}_2\text{-CH}_2\text{-CH}_3$)₄), 1.88–1.70 (m, 24H, H11), 1.66–1.61 (m, 8H, N-($\text{CH}_2\text{-CH}_2\text{-CH}_2\text{-CH}_3$)₄), 1.39–1.17 (m, 72H, H8, H9, H10), 0.95 (t, $J = 7.4$ Hz, 12H, N-($\text{CH}_2\text{-CH}_2\text{-CH}_2\text{-CH}_3$)₄); ^{13}C NMR (100 MHz, D_2O): δ (ppm) = 160.9, 159.9 (C16, C18), 145.4 (C14), 123.9 (C13), 78.9 (C4), 70.6 (C17), 69.9 (C3), 65.7 (C2), 58.7 ((N- $\text{CH}_2\text{-CH}_2\text{-CH}_2\text{-CH}_3$), 58.1 (C5), 56.0 (C6), 52.5 (C1), 50.9 (C7), 47.9 (C12, C19), 40.0 (C15), 30.0 (N- $\text{CH}_2\text{-CH}_2\text{-CH}_2\text{-CH}_3$), 26.8 (C11), 26.2 (C9), 23.8 (C10), 23.3 (C8), 19.8 (N- $\text{CH}_2\text{-CH}_2\text{-CH}_2\text{-CH}_3$), 13.4 (N- $\text{CH}_2\text{-CH}_2\text{-CH}_2\text{-CH}_3$); IR (neat, $\nu_{\text{max}}/\text{cm}^{-1}$) 3331 (OH), 2920 (CH_2), 1702 (NC=O), 1482 (CH_2), 1216 (C-N), 1067 (C-O); $[\alpha]_{\text{D}}^{20} = +4.2$ (c 0.12, H_2O).

3.1.16. Synthesis of Br⁻@(DNJ-C9)₁₂BU[6].TBA⁺ **10**

To a solution of anion-free (DNJ-C9)₁₂BU[6] **7** (10.8 mg, 2.02 μmol, 1 eq.) in H₂O (1 mL) was added a solution of TBABr in H₂O (63.6 μL, c = 31.8 μM/mL 1 eq.). The reaction mixture was sonicated for 30 min and then was lyophilized to afford Br⁻@(DNJ-C9)₁₂BU[6].TBA⁺ **10** (11.2 mg, 98% yield). ¹H NMR (400 MHz, D₂O/MeOD 0.35/0.2): δ (ppm) = 7.87 (br s, 12H, H16), 5.77 (br s, 12H, H20), 4.62–4.52 (m, 36H, H18, H22), 4.29–4.24 (m, 24H, H15), 3.85–3.81 (m, 24H, H6), 3.55–3.48 (m, 12H, H4), 3.37–3.33 (m, 12H, H2), 3.24–3.19 (m, 20H, H3, N-(CH₂-CH₂-CH₂-CH₃)₄), 2.98 (d, J = 6.7 Hz, 12H, H1a), 2.77–2.63 (m, 12H, H7a), 2.62–2.50 (m, 12H, H7b), 2.33–2.12 (m, 24H, H1b, H5), 1.82–1.78 (m, 24H, H14), 1.66–1.59 (m, 8H, N-(CH₂-CH₂-CH₂-CH₃)₄), 1.50–1.31 (m, 32H, H8, N-(CH₂-CH₂-CH₂-CH₃)₄), 1.25–1.16 (m, 120H, H9, H10, H11, H12, H13), 0.96 (t, J = 7.4 Hz, 12H, N-(CH₂-CH₂-CH₂-CH₃)₄); ¹³C NMR (176 MHz, D₂O/MeOD 0.35/0.2): δ (ppm) = 160.8, 160.0 (C19-C21), 145.9 (C17), 124.3 (C16), 79.5 (C4), 71.0 (C20), 69.9 (C2, C3), 66.4 (C5), 59.1 (N-CH₂-CH₂-CH₂-CH₃), 58.5 (C6), 56.7 (C1), 53.4 (C7), 51.3 (C22), 40.3 (C15, C18), 30.8 (C14), 30.0 (N-CH₂-CH₂-CH₂-CH₃), 29.5–28.0–27.0–24.3–23.9 (C8, C9, C10, C11, C12, C13), 20.3 (N-CH₂-CH₂-CH₂-CH₃), 13.9 ((N-CH₂-CH₂-CH₂-CH₃). IR (neat, ν_{max}/cm⁻¹) 3375 (OH), 2922 (CH₂), 1702 (NC=O), 1482 (CH₂), 1131 (C-N), 1057 (C-O). [α]_D²⁰ = + 3.8 (c 0.10, H₂O/MeOH 0.3/0.2).

3.1.17. Synthesis of Br⁻@(DNJ-OAc-Tripod)₆BU[6] Na⁺ **20**

To a solution of propargylated bambusuril **2** (6.0 mg, 3.53 μmol, 1 eq.) in H₂O/*t*BuOH (1.2 mL, 0.5/0.7) were added tripod-azide **14** (105.5 mg, 56.74 μmol, 16 eq.), sodium ascorbate (14.2 μL of 1 M aqueous solution, 14.20 μmol, 4 eq.) and copper sulfate (7.1 μL of 1 M aqueous solution, 7.10 μmol, 2 eq.). The reaction was stirred and heated under microwave irradiations for 3 h at 80 °C with a power of 50 W. A solution of MeCN/H₂O/NH₄OH (30w%) (1 mL, 15/0.5/0.5, *v/v/v*) was then added and the mixture was filtered on a small pad of SiO₂. The filtrate was concentrated under vacuum and the crude product was purified on silica gel chromatography (CH₂Cl₂/MeOH, 99:1 to 95:5) to afford Br⁻@(DNJ-OAc-Tripod)₆BU[6].Na⁺ **20** (37.5 mg, 84% yield). ¹H NMR (400 MHz, CDCl₃): δ (ppm) = 7.64–7.45 (m, 24H, H16, H26), 5.90–5.65 (br s, 12H, H33), 5.17–4.83 (m, 54H, H2, H3, H4), 4.55–4.22 (m, 120H, H15, H18, H25, H28, H30, H35), 4.18–4.10 (m, 36H, H6), 3.83–3.60 (m, 12H, H24), 3.48–3.28 (m, 72H, H19, H21, H22, H23), 3.24–3.10 (m, 18H, H1a), 2.80–2.47 (m, 54H, H5, H7), 2.38–2.25 (m, 18H, H1b), 2.11 (br s, 6H, H32), 2.10–1.88 (m, 252H, CH₃-C=O, H14), 1.85–1.74 (m, 36H, H8), 1.51–1.29 (m, 36H, H8), 1.29–1.19 (m, 180H, H9, H10, H11, H12, H13); ¹³C NMR (176 MHz, CDCl₃): δ (ppm) = 170.8, 170.3, 169.9, 169.7 (CH₃-C=O), 159.2 (C29, C34), 145.2 (C17, C27), 123.9 (C16), 122.9 (C26), 74.1 (C3), 71.2–70.3–69.9 (C21, C22, C23), 69.3 (C4, C24), 68.8 (C2, C19, C33), 65.0 (C18), 61.6 (C5), 58.9 (C6), 52.1 (C1), 50.4 (C7, C15, C25), 47.8 (C35), 45.5 (C20), 39.4 (C28), 30.5 (C14), 29.8, 29.4, 29.1, 27.1, 26.6 (C9, C10, C11, C12, C13), 24.3 (C8), 21.0, 20.9, 20.8, 20.7 (CH₃-C=O); IR (neat, ν_{max}/cm⁻¹) 2927 (CH₂), 1745 (CH₃-C=O), 1704 (NC=O), 1471 (C-N), 1225 (C-H), 1032 (C-O); HRMS (ESI⁺): *m/z* calculated for [C₅₈₈H₈₉₄N₁₁₄O₁₈₆+9H]⁹⁺: 1393.0446, found 1393.8317; [α]_D²⁰ = 9.9 (c 0.105, CHCl₃).

3.1.18. Synthesis of Br⁻@(DNJ-Tripod)₆BU[6].Na⁺ **11**

To a solution of Br⁻@(DNJ-OAc-Tripod)₆BU[6].Na⁺ **20** (19.5 mg, 1.54 μmol, 1 eq.) in H₂O/MeOH (1 mL 1/1), amberlite IRN 78 (HO⁻) (59 mg) was added and the mixture was heated at 40 °C for 12 h. After concentration under vacuum, Br⁻@(DNJ-Tripod)₆BU[6].Na⁺ **11** was obtained (12.5 mg, 84% yield). ¹H NMR (D₂O/MeOD 50/50, 400 MHz): δ (ppm) 7.94 (br s, 24H, H16, H26), 5.96–5.77 (m, 12H, H33), 4.50–4.26 (m, 90H, H2, H3, H4, H25, H28, H30), 3.85 (br s, 36H, H18), 3.69 (s, 12H, H35), 3.59–3.51 (m, 36H, H15), 3.43–3.28 (m, 84H, H19, H21, H22, H23, H24), 3.22 (t, J = 9.0 Hz, 36H, H6), 3.03–2.98 (m, 18H, H1a), 2.79–2.69 (m, 18H, H7a), 2.68–2.56 (m, 18H, H7b), 2.27–2.16 (m, 42H, H1, H5, H32), 1.86–1.78 (m, 36H, H14), 1.51–1.35 (m, 36H, H8), 1.37–1.11 (m, 180H, H9, H10, H11, H12, H13); ¹³C NMR (176 MHz, D₂O/MeOD 50/50): δ (ppm) 159.4 (C29, C34), 145.6 (C17, C27), 125.2 (C16, C26), 79.7 (C3), 71.2 (C21, C22, C23), 70.0 (C4), 69.5 (C24), 66.4 (C2, C19, C33), 64.9 (C18),

58.7 (C5), 56.8 (C6), 53.4 (C1), 51.3 (C7, C15, C25), 46.1 (C35), 45.2 (C20), 40.1 (C28), 30.9 (C14), 30.1, 29.9, 29.6, 28.2, 27.1 (C9, C10, C11, C12, C13), 24.1 (C8); IR (neat, $\nu_{\max}/\text{cm}^{-1}$): 3550 (OH), 2922 (CH₂), 1702 (NC=O), 1394 (C-N), 1249 (CH), 1065 (C-O); $[\alpha]_{\text{D}}^{20} = +1.8$ (c 0.055, H₂O/MeOH 1/1); HRMS MS(ESI+): m/z calculated for (C₄₄₄H₇₅₀N₁₁₄O₁₁₄+13H)¹³⁺: 732.0492, found 732.8294.

3.2. Isothermal Titration Calorimetry Experiments

ITC measurements were performed with a VP-ITC microcalorimeter (Microcal, GE-Healthcare). Experiments were carried out in water and in a solution of K₂HPO₄ (1.5 mM) in milli-Q water at 298.15 ± 0.1 K. Anion binding to BU was investigated via a classical isothermal titration experiment (10 µL additions) and a single injection method (SIM). Injection of sodium iodide solution was added automatically to the BU solution present in the calorimeter cell while stirring at 307 rpm. Integrated heat effects were analyzed by non-linear regression using a single-site binding model (Microcal Origin 7). The experimental data fitted to a theoretical titration curve, giving the association constant K_a , the enthalpy of binding ΔH° and the entropy ΔS° . The free energy ΔG° was calculated from the equation: $\Delta G^\circ = \Delta H^\circ - T\Delta S^\circ$, where T is the absolute temperature. The first smaller addition (2 µL), which was used to compensate for diffusion of the guest from the injector during equilibration, was discarded prior to data fitting.

3.3. Inhibition Assays on Jack-Bean α -Mannosidase

p-nitrophenyl- α -D-mannopyranoside and α -mannosidase (EC 3.2.1.24, from Jack Bean) were purchased from Sigma Aldrich, St. Louis, MO, USA. Inhibition constants were determined spectrophotometrically by measuring the residual hydrolytic activities of the α -mannosidase against *p*-nitrophenyl- α -D-mannopyranoside in the presence and absence of an inhibitor. Each well was filled with a total volume of 100 µL, containing 0.2 M acetate buffer pH 5, inhibitor, substrate and enzyme. All kinetics were performed between 25 °C and 27 °C and started by enzyme addition. After 30–50 min of incubation, the reaction was quenched by addition of 100 µL of 1M Na₂CO₃. The absorbance of the resulting solution was determined at 405 nm. K_i values were determined in triplicate, using the Dixon and Lineweaver–Burk graphical methods within Microsoft Excel. Stock solutions of inhibitors were prepared with DMSO/buffer for final well DMSO content under 5%. The stability of the enzyme in the presence of the same concentrations of DMSO was controlled and enzyme activity was unaffected.

4. Conclusions

Propargylated bambus[4,6]urils were fully functionalized by click chemistry with linear *N*-alkylDNJ ligands either having 6 or 9 carbon alkyl azido linkers or a trivalent DNJ derivative to generate multivalent clusters bearing up to 24 iminosugars. The novelty of this study lies in the unique combination of anion-transporting BU[6] scaffolds with iminosugar inhitopes that have already proven their efficiency towards the multivalent inhibition of glycosidases. For clusters grafted with DNJ ligands linked by short C6 arms, scaffold size showed a strong impact on α -mannosidase inhibition, with the best results obtained for BU[4] clusters. With nonyl chains, the enzyme affinity per inhibitory head increases drastically whichever platform is used, the best affinity increases being obtained with trivalent dendrons providing higher local inhibitor concentration. Bromide and iodide sequestered in BU[6] grafted by DNJ inhibitors were also prepared and their activity was compared to their corresponding anion-free counterparts, showing that the presence of anions neither modified the inhibition potency of the clusters nor their inhibition mode. Our study thus shows a first proof of concept for glycosidase-directed ion caging agents based on unprecedented bambusuril-based iminosugar clusters. Altogether, these results open the way to unique water-soluble probes/therapeutic agents with both strong glycosidase inhibition potency and ion receptor properties.

Supplementary Materials: The following supporting information can be downloaded at: <https://www.mdpi.com/article/10.3390/molecules27154772/s1>, Figure S1: NMR ^1H and ^{13}C spectra of compounds 3, 4, 5, 6, 7, 8, 9, 10, 11, 15, 16, 17, 18, 19, 20, ITC of Γ binding to 6 and enzymatic study of 3, 4, 5, 6, 8, 9, 10 and 11.

Author Contributions: M.L., J.P.S., Y.L. and E.C. synthesized the compounds. M.L., J.P.S. and A.B. performed the enzymatic studies. M.L. and E.C. performed the ITC experiments. M.-P.H., P.C. and A.B. designed the project, analyzed the results and wrote the manuscript. All authors have read and agreed to the published version of the manuscript.

Funding: This work was funded by the CEA (Commissariat à l’Energie Atomique) through fellowships for M.L. and E.C. and the International Centre for Frontier Research in Chemistry (icFRC) through a fellowship provided to J.P.S.; Y.L. is grateful to the Chinese Scholarship Council (CSC) for a PhD fellowship. The authors also acknowledge financial support from the University of Strasbourg and the CNRS (LIMA-UMR 7042).

Institutional Review Board Statement: Not applicable.

Informed Consent Statement: Not applicable.

Data Availability Statement: Not applicable.

Acknowledgments: We thank J. Rivollier (Université Paris-Saclay/CEA/DMTS/SCBM) for preliminary neoglycoBUs synthesis. Y. Boulard (Université Paris-Saclay/CEA/I2BC) and F. Fenaille (Université Paris-Saclay/CEA/DMTS/SPI) are thanked for recording 600 MHz NMR spectra and for mass spectrometry experiments, respectively.

Conflicts of Interest: The authors declare no conflict of interest.

References

1. Svec, J.; Necas, M.; Sindelar, V. Bambus[6]uril. *Angew. Chem. Int. Ed.* **2010**, *49*, 2378–2381. [[CrossRef](#)] [[PubMed](#)]
2. Lizal, T.; Sindelar, V. Bambusuril Anion Receptors. *Isr. J. Chem.* **2018**, *58*, 326–333. [[CrossRef](#)]
3. Mondal, P.; Solel, E.; Mitra, S.; Keinan, E.; Reany, O. Equatorial Sulfur Atoms in Bambusurils Spawn Cavity Collapse. *Org. Lett.* **2020**, *22*, 204–208. [[CrossRef](#)] [[PubMed](#)]
4. Havel, V.; Sindelar, V. Anion Binding Inside a Bambus[6]Uril Macrocycle in Chloroform. *Chem. Plus. Chem.* **2015**, *80*, 1601–1606. [[CrossRef](#)] [[PubMed](#)]
5. Havel, V.; Yawer, M.A.; Sindelar, V. Real-Time Analysis of Multiple Anion Mixtures in Aqueous Media Using a Single Receptor. *Chem. Commun.* **2015**, *51*, 4666–4669. [[CrossRef](#)]
6. Lang, C.; Mohite, A.; Deng, X.; Yang, F.; Dong, Z.; Xu, J.; Liu, J.; Keinan, E.; Reany, O. Semithiobambus[6]Uril Is a Transmembrane Anion Transporter. *Chem. Commun.* **2017**, *53*, 7557–7560. [[CrossRef](#)]
7. Valkenier, H.; Akrawi, O.; Jurček, P.; Sleziačková, K.; Lizal, T.; Bartik, K.; Šindelář, V. Fluorinated Bambusurils as Highly Effective and Selective Transmembrane $\text{Cl}^-/\text{HCO}_3^-$ Antiporters. *Chemistry* **2019**, *5*, 429–444. [[CrossRef](#)]
8. Šlampová, A.; Šindelář, V.; Kubáň, P. Application of a Macrocylic Compound, Bambus[6]Uril, in Tailor-Made Liquid Membranes for Highly Selective Electromembrane Extractions of Inorganic Anions. *Anal. Chim. Acta* **2017**, *950*, 49–56. [[CrossRef](#)]
9. Vázquez, J.; Šindelář, V. Phase-Transfer Extraction for the Fast Quantification of Perchlorate Anions in Water. *RSC Adv.* **2019**, *9*, 35452–35455. [[CrossRef](#)]
10. Maršálek, K.; Šindelář, V. Monofunctionalized Bambus[6]urils and Their Conjugates with Crown Ethers for Liquid–Liquid Extraction of Inorganic Salts. *Org. Lett.* **2020**, *22*, 1633–1637. [[CrossRef](#)]
11. Fiala, T.; Ludvíková, L.; Heger, D.; Švec, J.; Slanina, T.; Vetráková, L.; Babiak, M.; Nečas, M.; Kulhánek, P.; Klán, P.; et al. Bambusuril as a One-Electron Donor for Photoinduced Electron Transfer to Methyl Viologen in Mixed Crystals. *J. Am. Chem. Soc.* **2017**, *139*, 2597–2603. [[CrossRef](#)] [[PubMed](#)]
12. Rivollier, J.; Thuery, P.; Heck, M.-P. Extension of the Bambus[n]uril Family: Microwave Synthesis and Reactivity of Allylbambus[n]urils. *Org. Lett.* **2013**, *15*, 480–483. [[CrossRef](#)] [[PubMed](#)]
13. Azazna, D.; Lafosse, M.; Rivollier, J.; Wang, J.; Ben Cheikh, I.; Meyer, M.; Thuéry, P.; Dognon, J.-P.; Huber, G.; Heck, M.-P. Functionalization of Bambusurils by a Thiol–Ene Click Reaction and a Facile Method for the Preparation of Anion-Free Bambus[6]urils. *Chem.–Eur. J.* **2018**, *24*, 10793–10801. [[CrossRef](#)]
14. Lafosse, M.; Cartier, E.; Solmont, K.; Rivollier, J.; Azazna, D.; Thuéry, P.; Boulard, Y.; Gontier, A.; Charbonnier, J.-B.; Kuhnast, B.; et al. Clickable Bambusurils to Access Multivalent Architectures. *Org. Lett.* **2020**, *22*, 3099–3103. [[CrossRef](#)] [[PubMed](#)]
15. Compain, P.; Bodlenner, A. The multivalent effect in glycosidase inhibition: A new, rapidly emerging topic in glycoscience. *ChemBioChem* **2014**, *15*, 1239–1251. [[CrossRef](#)] [[PubMed](#)]
16. Gouin, S.G. Multivalent inhibitors for carbohydrate-processing enzymes: Beyond the “lock-and-key” concept. *Chem.–Eur. J.* **2014**, *20*, 11616–11628. [[CrossRef](#)]

17. Zelli, R.; Longevial, J.-F.; Dumy, P.; Marra, A. Synthesis and biological properties of multivalent iminosugars. *New J. Chem.* **2015**, *30*, 5050–5074. [[CrossRef](#)]
18. Matassini, C.; Parmeggiani, C.; Cardona, F.; Goti, A. Are enzymes sensitive to the multivalent effect? Emerging evidence with glycosidases. *Tetrahedron Lett.* **2016**, *57*, 5407–5415. [[CrossRef](#)]
19. González-Cuesta, M.; Ortiz Mellet, C.; García Fernández, J.M. Carbohydrate supramolecular chemistry: Beyond the multivalent effect. *Chem. Commun.* **2020**, *56*, 5207–5222. [[CrossRef](#)]
20. Compain, P. Multivalent effect in glycosidase inhibition: The end of the beginning. *Chem. Rec.* **2020**, *20*, 10–22. [[CrossRef](#)]
21. Diot, J.; García-Moreno, M.I.; Gouin, S.G.; Ortiz Mellet, C.; Haupt, K.; Kovensky, J. Multivalent iminosugars to modulate affinity and selectivity for glycosidases. *Org. Biomol. Chem.* **2009**, *7*, 357–363. [[CrossRef](#)] [[PubMed](#)]
22. Compain, P.; Decroocq, C.; Iehl, J.; Holler, M.; Hazelard, D.; Mena Barragán, T.; Ortiz Mellet, C.; Nierengarten, J.-F. Glycosidase Inhibition with Fullerene Iminosugar Balls: A Dramatic Multivalent Effect. *Angew. Chem. Int. Ed.* **2010**, *49*, 5753–5756. [[CrossRef](#)] [[PubMed](#)]
23. Vanni, C.; Bodlenner, A.; Marradi, M.; Schneider, J.P.; de los Angeles Ramirez, M.; Moya, S.; Goti, A.; Cardona, F.; Compain, P.; Matassini, C. Hybrid Multivalent Jack Bean α -Mannosidase Inhibitors: The First Example of Gold Nanoparticles Decorated with Deoxynojirimycin Inhibitors. *Molecules* **2021**, *26*, 5864. [[CrossRef](#)]
24. Bonduelle, C.; Huang, J.; Mena-Barragán, T.; Ortiz Mellet, C.; Decroocq, C.; Etamé, E.; Heise, A.; Compain, P.; Lecommandoux, S. Iminosugar-based glycopolyptides: Glycosidase inhibition with bioinspired glycoprotein analogue micellar selfassemblies. *Chem. Commun.* **2014**, *50*, 3350–3352. [[CrossRef](#)] [[PubMed](#)]
25. Brissonnet, Y.; Ortiz Mellet, C.; Morandat, S.; Garcia-Moreno, M.I.; Deniaud, D.; Matthews, S.E.; Vidal, S.; Sesták, S.; El Kirat, K.; Gouin, S.G. Topological Effects and Binding Modes Operating with Multivalent Iminosugar-Based Glycoclusters and Mannosidases. *J. Am. Chem. Soc.* **2013**, *135*, 18427–18435. [[CrossRef](#)]
26. Lepage, M.L.; Schneider, J.P.; Bodlenner, A.; Meli, A.; De Riccardis, F.; Schmitt, M.; Tarnus, C.; Nguyen-Huynh, N.-T.; Francois, Y.-N.; Leize-Wagner, E.; et al. Iminosugar-Cyclopeptoid Conjugates Raise Multivalent Effect in Glycosidase Inhibition at Unprecedented High Levels. *Chem.–Eur. J.* **2016**, *22*, 5151–5155. [[CrossRef](#)]
27. Assailly, C.; Bridot, C.; Saumonneau, A.; Lottin, P.; Roubinet, B.; Krammer, E.-M.; François, F.; Vena, F.; Landemarre, L.; Alvarez Dorta, D.; et al. Polyvalent Transition-State Analogues of Sialyl Substrates Strongly Inhibit Bacterial Sialidases. *Chem.–Eur. J.* **2021**, *27*, 3142–3150. [[CrossRef](#)]
28. Alvarez-Dorta, D.; Brissonnet, Y.; Saumonneau, A.; Deniaud, D.; Bernard, J.; Yan, X.; Tellier, C.; Daligault, F.; Gouin, S. Magnetic Nanoparticles Coated with Thiomannosides or Iminosugars to Switch and Recycle Galactosidase Activity. *Chem. Sel.* **2017**, *2*, 9552–9556. [[CrossRef](#)]
29. Brissonnet, Y.; Ladevèze, S.; Tezé, D.; Fabre, E.; Deniaud, D.; Daligault, F.; Tellier, C.; Šesták, S.; Remaud-Simeon, M.; Potocki-Veronese, G.; et al. Polymeric Iminosugars Improve the Activity of Carbohydrate-Processing Enzymes. *Bioconjug. Chem.* **2015**, *26*, 766–772. [[CrossRef](#)]
30. Ding, F.; Songkiatasak, P.; Cherukuri, P.K.; Huang, T.; Xu, X.-H.N. Size-Dependent Inhibitory Effects of Antibiotic Drug Nanocarriers against *Pseudomonas Aeruginosa*. *ACS Omega* **2018**, *3*, 1231–1243. [[CrossRef](#)]
31. Durka, M.; Buffet, K.; Iehl, J.; Holler, M.; Nierengarten, J.-F.; Vincent, S.P. The Inhibition of Liposaccharide Heptosyltransferase WaaC with Multivalent Glycosylated Fullerenes: A New Mode of Glycosyltransferase Inhibition. *Chem.–Eur. J.* **2012**, *18*, 641–651. [[CrossRef](#)] [[PubMed](#)]
32. Hurtaux, T.; Sfihi-Loualia, G.; Brissonnet, Y.; Bouckaert, J.; Mallet, J.-M.; Sendid, B.; Delplace, F.; Fabre, E.; Gouin, S.G.; Guérardel, Y. Evaluation of Monovalent and Multivalent Iminosugars to Modulate *Candida Albicans* β -1,2-Mannosyltransferase Activities. *Carbohydr. Res.* **2016**, *429*, 123–127. [[CrossRef](#)] [[PubMed](#)]
33. Tikad, A.; Fu, H.; Sevrain, C.M.; Laurent, S.; Nierengarten, J.-F.; Vincent, S.P. Mechanistic Insight into Heptosyltransferase Inhibition by Using Kdo Multivalent Glycoclusters. *Chem.–Eur. J.* **2016**, *22*, 13147–13155. [[CrossRef](#)] [[PubMed](#)]
34. Ismail, C.; Nocentini, A.; Supuran, C.T.; Winum, J.-Y.; Gharbi, R. 1,5-Benzodiazepines as a Platform for the Design of Carbonic Anhydrase Inhibitors. *Arch. Pharm.* **2022**, *355*, 2100405. [[CrossRef](#)] [[PubMed](#)]
35. Mammen, M.; Choi, S.-K.; Whitesides, G.M. Polyvalent Interactions in Biological Systems: Implications for Design and Use of Multivalent Ligands and Inhibitors. *Angew. Chem. Int. Ed.* **1998**, *37*, 2754–2794. [[CrossRef](#)]
36. Howard, E.; Cousido-Siah, A.; Lepage, M.L.; Schneider, J.P.; Bodlenner, A.; Mitschler, A.; Meli, A.; Izzo, I.; Alvarez, H.A.; Podjarny, A.; et al. Structural Basis of Outstanding Multivalent Effects in Jack Bean α -Mannosidase Inhibition. *Angew. Chem. Int. Ed.* **2018**, *57*, 8002–8006. [[CrossRef](#)] [[PubMed](#)]
37. Decroocq, C.; Rodríguez-Lucena, D.; Russo, V.; Mena Barragán, T.; Ortiz Mellet, C.; Compain, P. The Multivalent Effect in Glycosidase Inhibition: Probing the Influence of Architectural Parameters with Cyclodextrin-Based Iminosugar Click Clusters. *Chem.–Eur. J.* **2011**, *17*, 13825–13831. [[CrossRef](#)]
38. Joosten, A.; Schneider, J.P.; Lepage, M.L.; Tarnus, C.; Bodlenner, A.; Compain, P. A Convergent Strategy for the Synthesis of Second-Generation Iminosugar Clusters Using “Clickable” Trivalent Dendrons: Synthesis of Second-Generation Iminosugar Clusters. *Eur. J. Org. Chem.* **2014**, *2014*, 1866–1872. [[CrossRef](#)]
39. Decroocq, C.; Joosten, A.; Sergent, R.; Mena Barragán, T.; Ortiz Mellet, C.; Compain, P. The Multivalent Effect in Glycosidase Inhibition: Probing the Influence of Valency, Peripheral Ligand Structure, and Topology with Cyclodextrin-Based Iminosugar Click Clusters. *ChemBioChem* **2013**, *14*, 2038–2049. [[CrossRef](#)]

40. Pathak, V.P. A Convenient Method for O-Deacetylation Using IRA-400(OH) Resin. *Synth. Commun.* **1993**, *23*, 83–85. [[CrossRef](#)]
41. Nierengarten, J.-F.; Schneider, J.P.; Nguyet Trinh, T.M.; Joosten, A.; Holler, M.; Lepage, M.L.; Bodlener, A.; Garcia-Moreno, M.I.; Ortiz Mellet, C.; Compain, P. Giant Glycosidase Inhibitors: First- and Second-Generation Fullerodendrimers with a Dense Iminosugar Shell. *Chem.–Eur. J.* **2018**, *24*, 2483–2492. [[CrossRef](#)] [[PubMed](#)]
42. Havel, V.; Svec, J.; Wimmerova, M.; Dusek, M.; Pojarova, M.; Sindelar, V. Bambus[n]-urils: A New Family of Macrocyclic Anion Receptors. *Org. Lett.* **2011**, *13*, 4000–4003. [[CrossRef](#)] [[PubMed](#)]
43. Schneider, J.P.; Tommasone, S.; Della Sala, P.; Gaeta, C.; Talotta, C.; Tarnus, C.; Neri, P.; Bodlener, A.; Compain, P. Synthesis and Glycosidase Inhibition Properties of Calix[8]Arene-Based Iminosugar Click Clusters. *Pharmaceuticals* **2020**, *13*, 366. [[CrossRef](#)]
44. Tranoy-Opalinski, I.; Legigan, T.; Barat, R.; Clarhaut, J.; Thomas, M.; Renoux, B.; Papot, S. β -Glucuronidase-responsive Prodrugs for Selective Cancer Chemotherapy: An Update. *Eur. J. Med. Chem.* **2014**, *74*, 302–313. [[CrossRef](#)]
45. Mayson, S.E.; Chan, C.M.; Haugen, B.M. Tailoring the Approach to Radioactive Iodine Treatment in Thyroid Cancer. *Endocr.-Relat. Cancer* **2021**, *28*, T125–T140. [[CrossRef](#)] [[PubMed](#)]
46. Tian, Q.; Zhu, H.H.; Li, H. Interstitial brachytherapy of oral squamous cell carcinoma with ultrasound-guided iodine-125 radioactive seed implantation. *Eur. Rev. Med. Pharm. Sci.* **2018**, *22*, 1680–1685. [[CrossRef](#)]
47. Juweid, M.E.; Sharkey, R.M.; Behr, T.; Swayne, L.C.; Dunn, R.; Siegel, J.; Goldenberg, D.M. Radioimmunotherapy of patients with small-volume tumors using iodine-131-labeled anti-CEA monoclonal antibody NP-4 F(ab')(2). *J. Nucl. Med.* **1996**, *37*, 1504–1510.